Computer Simulation of the Dynamics of a Single Polymer Chain

David Ceperley[a] and M. H. Kalos

Courant Institute of Mathematical Sciences, New York University, New York, New York 10012

and

Joel L. Lebowitz

Department of Mathematics and Physics, Rutgers University, New Brunswick, New Jersey 08903
(Received 17 May 1978)

We have carried out computer simulations of the dynamics of a model polymer chain in a solvent. We find that the structure function scales for different chain sizes N as a function of $q = kN^\nu$ with $\nu = 0.6 \simeq$ exponent for the radius of gyration. Furthermore, $S(q) \sim q^{-5/3}$ over a wide range, as predicted by Edwards. Time-dependent correlation functions appear to scale as tN^α, with $\alpha \simeq 2\nu + 1$. The time-displaced structure function is of the form $S(kN^\nu, tN^\alpha)$.

Computer calculations, and in particular Monte Carlo methods, have been used previously to find the equilibrium properties of a single chain in a solvent. It was found, for example, that if there are excluded-volume interactions between elements of the chain, then the size of the chain grows as N^ν, where N is the number of beads and $\nu \simeq 0.6$, in agreement with theories proposed by Flory,[1] Yamakawa,[2] Domb,[3] and de Gennes.[4] Dynamical calculations of large polymers have thus far been confined to lattice models[5] which have been criticized as being too dependent upon the rules for jumping.[6] Indeed, it is not at all apparent that a lattice model can represent the dynamics of a real polymer since many of the important motions may be small bending and stretching movements and not discontinuous jumps.

We have chosen the "bead-spring" model to represent the polymer chain: "N" beads with coordinates $R = \{\vec{r}_i : 1 \le i \le N\}$, connected by harmonic springs. A repulsive, short-range, excluded-volume interaction $\Phi(r_{ij})$ acts between all pairs of beads. The total potential energy of the chain is

$$U(R) = \sum_{i=1}^{N-1} \tfrac{1}{2}\kappa(\vec{r}_i - \vec{r}_{i+1})^2 + \sum_{i<j} \Phi(|\vec{r}_i - \vec{r}_j|), \quad (1)$$

$$\Phi(r) = \begin{cases} 4\epsilon[(\sigma/r)^{12} - (\sigma/r)^6 + \tfrac{1}{4}], & r \le 2^{1/6}\sigma, \\ 0, & r \ge 2^{1/6}\sigma. \end{cases} \quad (2)$$

The potential of Eq. (2) is stiff enough for small r_{ij} that the "excluded volume" depends weakly on ϵ; $\epsilon = 0$ corresponds to the Rouse-Zimm model.

Following the work of Kirkwood[7] and Rouse[8] we assume that the velocity of the polymer is proportional to the forces acting on it at any time; this is the high-viscosity limit in which inertial terms are neglected. Neglecting also hydrody-

namic forces, we then have for the velocity of the jth bead at time t

$$\vec{v}_j(t) = -\beta D \nabla_j U(R) + \vec{W}(t). \quad (3)$$

Here β is the reciprocal temperature of the solvent, D is the diffusion constant of a monomer, and W is a Gaussian fluctuating "Langevin force" (due to the solvent) with mean $\langle W(t)\rangle = 0$ and covariance $\langle \vec{W}(t_1) \cdot \vec{W}(t_2)\rangle = 6D\delta(t_1 - t_2)$. This leads to the Smoluchowski equation for the time evolution of the polymer probability density $f(R,t)$,

$$\frac{\partial f(R,t)}{\partial t}$$
$$= D\sum_{j=1}^{N} \nabla_j \cdot [\nabla_j f(R,t) + \beta f(R,t)\nabla_j U(R)]. \quad (4)$$

The solution of (3) approaches equilibrium as $t \to \infty$; $f(R,t) \to Z^{-1}e^{-U(R)}$.

The solution of the diffusion equation (4) was generated by a Monte Carlo random walk: Full details will be given elsewhere. We mention here only that our basic time step was chosen to be $\tau = 0.01$ in units of σ^2/D; distances were measured in units of σ, and we set $\beta\kappa = 2$, $\beta\epsilon = 0.1$. Both static and dynamic results given below correspond to equilibrium ensemble averages and are denoted by $\langle \ldots \rangle$.

The mean-square end-to-end vector

$$\vec{L} = \vec{r}_N - \vec{r}_1, \quad (5)$$

and the radius of gyration

$$G^2 = \frac{1}{N}\sum_{i=1}^{N} (\vec{r}_i - \vec{Z})^2,$$

$\vec{Z}$ the center of mass, are given in Table I. Within statistical errors $G^2 = 0.3N^{1.2}$ and $L^2 = 6G^2$.

TABLE I. Static properties of our model. N is the number of beads, T is the total simulation time (in units of σ^2/D), $\vec{L}$ is the end-to-end vector, G is the radius of gyration, and $R_1{}^2$ and $R_2{}^2$ are the smallest and second eigenvalues of the moment of inertia tensor.

N	T	$\langle L^2 \rangle$	$\langle G^2 \rangle$	$\langle R_1{}^2 \rangle / \langle G^2 \rangle$	$\langle R_2{}^2 \rangle / \langle G^2 \rangle$
5	5×10^3	10.35 ± 0.05	1.929 ± 0.012	0.037	0.166
10	5×10^3	27.8 ± 0.3	4.65 ± 0.04	0.051	0.159
20	7.5×10^3	70 ± 4	11.0 ± 0.5	0.053	0.157
33	10^4	125 ± 6	19.9 ± 0.6	0.054	0.162
48	11×10^4	197 ± 14	31 ± 1.5	0.057	0.176
63	8×10^3	321 ± 40	48.6 ± 5	0.050	0.157

The moment of inertia tensor is defined by

$$T_{ab} = \frac{1}{N} \sum_{i=1}^{N} (r_i - Z)_a (r_i - Z)_b. \tag{6}$$

The eigenvalues of this tensor are measures of the instantaneous "width" of the polymer in the three orthogonal principal axes, ordered so that $R_1{}^2 \le R_2{}^2 \le R_3{}^2$. The average values of $R_i{}^2$ are given in Table I. It is striking that the ratios $\langle R_i{}^2 \rangle / \langle G^2 \rangle$ depend hardly at all on the number of beads, and are almost identical with those found in a nonintersecting random walk on a lattice.[9]

The structure function[2] is defined as

$$S(k) = \langle |\rho_k(R)|^2 \rangle \equiv \left\langle \left| \frac{1}{N} \sum_{i=1}^{N} \exp(i\vec{k} \cdot \vec{r}_i) \right|^2 \right\rangle. \tag{7}$$

For small k, one gets the Debye moment expansion[10]

$$S(k) = 1 - G^2 k^2 / 3 + O(k^4), \quad kG < 1. \tag{8}$$

For intermediate k, $1/G \le k \le 2$, the excluded-volume interaction causes the scattering function[11,12] to behave like $k^{-5/3}$. For large k the particles are uncorrelated and $S(k) \to 1/N$. Plotted in Fig. 1 is $S(q)$ versus $\log q$, $q = k\sigma N^{0.6}$. The remarkable insensitivity to the number of beads indicates that even ten beads is near the scaling limit as long as the probe looks at distances larger than σ (i.e., if $k < 2/\sigma$).

If $g(R)$ is some property which depends on the configuration of the polymer then the autocorre-
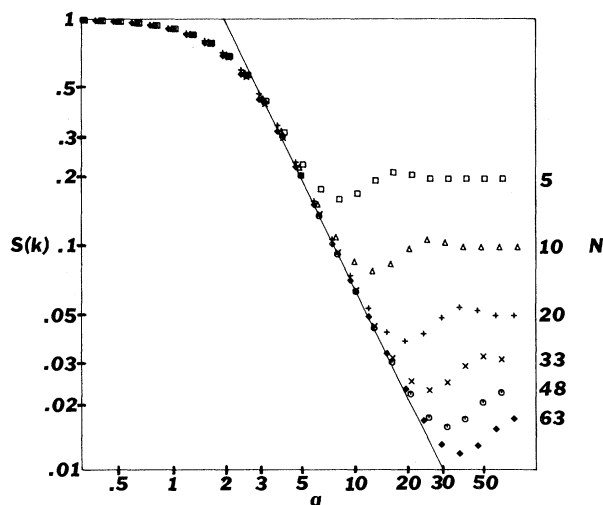
FIG. 1. $S_N(k)$ vs q, where $q = k\sigma N^{-\nu}$ and $\nu = 0.6$. The symbols represent the results of six different values of N (see right-hand scale). The line is $0.3q^{-5/3}$. For large k, $S(k) \to 1/N$. It is seen that for $k\sigma < 2$ the curves coincide.
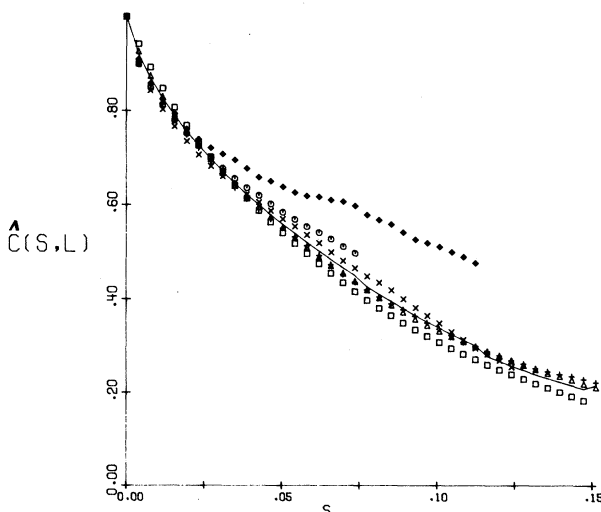
FIG. 2. $\hat{C}(s; \vec{L})$ vs s. The symbols are the correlation functions [i.e., $C_N(sN^\alpha; \vec{L})$] for six values of N (see Fig. 1 for key). With $\alpha = 2.13$ the solid line is the average of $C_N(sN^\alpha; \vec{L})$. The lozenges describe $N = 63$ for which the statistical errors are large enough to encompass the departure from the other curves.

TABLE II. Properties of the time-dependent correlation functions. α is the scaling exponent in Eq. (10) determined by least squares. $\bar{\tau}$ is the average relaxation rate [Eq. (12)]. τ_i and a_i are the relaxation rates and coefficients in Eq. (11) determined from least-squares fits to the scaled correlation functions. Time is in units of σ^2/D.

Function	α	$\bar{\tau}$	a_1	τ_1	a_2	τ_2
$\hat{C}(s;\vec{L})$	2.13 ± 0.05	0.069	0.91	0.096	0.08	0.0060
$C(s;R_3^2)$	2.22 ± 0.06	0.020	0.82	0.023	0.19	0.0059
$C(s;R_2^2)$	2.04 ± 0.03	0.0075	0.37	0.013	0.64	0.0040
$C(s;G^2)$	2.21 ± 0.06	0.020	0.76	0.024	0.24	0.0056
$\hat{F}(s,2)$	2.22 ± 0.03	0.25	0.97	0.25	0.03	0.020
$\hat{F}(s,4)$	2.24 ± 0.02	0.048	0.59	0.068	0.36	0.018
$\hat{F}(s,6)$	2.11 ± 0.02	0.019	0.47	0.032	0.49	0.0074
$\hat{F}(s,8)$	2.12 ± 0.02	0.0067	0.36	0.013	0.55	0.0032
$\hat{F}(s,10)$	2.08 ± 0.03	0.0038	0.32	0.0080	0.59	0.0019

lation function of g for a polymer of size N is

$$C_N(t;g) = \frac{\langle g^*(t_0)g(t_0+t)\rangle - |\langle g(t_0)\rangle|^2}{\langle |g(t_0)|^2\rangle - |\langle g(t_0)\rangle|^2}. \quad (9)$$

The autocorrelations for $\vec{L}$, L^2, G^2, and R_i^2 for different values of N appear to scale as

$$\hat{C}(s;g) \simeq C_N(sN^\alpha;g). \quad (10)$$

Here α is that exponent which brings the correlation functions deduced from the computer experiments into least-squares agreement. Shown in Fig. 2 are $\hat{C}(s;\vec{L})$ and $C_N(sN^\alpha;\vec{L})$ with $\alpha = 2.10 \pm 0.05$. The optimal values for α for the different correlation functions are given in Table II; it is seen that they are all between 2.04 and 2.24. All of the correlation functions seem to be a sum of exponentials as they are in the Rouse model[2]:

$$\hat{C}(s;g) = \sum a_i \exp(-s/\tau_i). \quad (11)$$

Included in Table II are the parameters of a two-exponential fit and the mean relaxation time

$$\bar{\tau} = \int_0^\infty \hat{C}(s;g)ds. \quad (12)$$

The lattice-dynamical simulations of Kranbuehl and Verdier[13] had a much higher value for the scaling exponent, namely $\alpha \simeq 3$. It was observed by Hilhorst and Deutch[6] that the transition rules in the lattice model contain subtle constraints which lead to a slowed relaxation. Our exponents lie close to the predictions of de Gennes[4] that $\alpha = 2\nu + 1$ but cannot be distinguished from renormalization predictions.[14] However, as seen in Table II, there are deviations from universality in the exponents, which may be a consequence of varying departures from scaling at small N for different functions g. For the Rouse model[8] $\alpha = 2$.

We have also computed the time-displaced scattering functions for chains of different sizes and found that these can be brought into a universal form when both k and t are scaled. The function

$$\hat{F}(s,q) = \langle \rho_k(t_0+t)\rho_k(t_0)\rangle,$$

where $k = qN^{-\nu}$ and $t = sN^\alpha$, is plotted in Fig. 3 for three values of q (2,4,6). In this figure $\nu = 0.6$ and α was obtained by a least-squares fit at each value of q. Table II contains $\alpha(q)$ as well as $a_i(q)$ and $\tau_i(q)$. The exponents α for small q are very close to $2\nu + 1$ and the scattering function is dominated by the diffusive motion of the center of mass $(\tau_1 \approx q^{-2})$. At larger values of q there appears to be a systematic decrease in the expon-
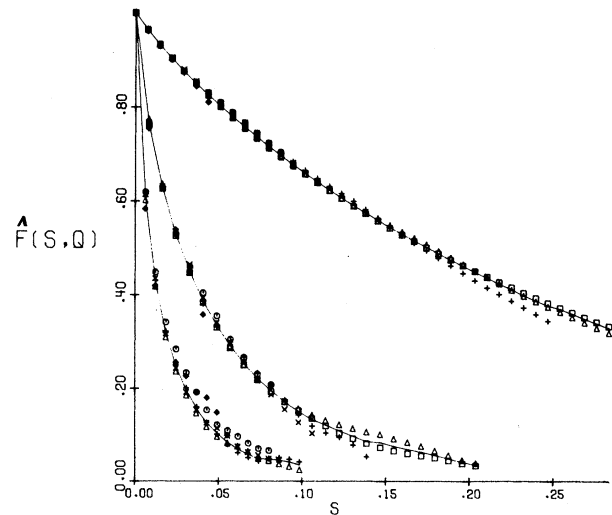

FIG. 3. $\hat{F}(s,q)$ vs s for three values of q (2,4,6). The symbols represent $F_N(sN^\alpha, qN^{-\nu})$ where $\nu = 0.6$ and $\alpha(q)$ is given in Table II. See key in Fig. 1. The line represents the average $\hat{F}(s,q)$.

315

ent ν and the relaxation times decrease faster than q^{-2}.

We would like to thank P. G. de Gennes, J. des Cloiseaux, G. Jannick, Marvin Bishop, Thomas C. Collins, and K. Binder for useful conversations. This work was supported in part by the U. S. Air Force Office of Scientific Research, Grant No. 78-3522, and in part by the U. S. Department of Energy, Grant No. EY-76-C-02-3077*000.

[a] Part of this work was done while the author was at the Department of Mathematics, Rutgers University. Present address: NRCC, Lawrence Berkeley Laboratory, Berkeley, Calif., 94720.

[1] P. J. Flory, *Principles of Polymer Chemistry* (Cornell Univ. Press, Ithaca, N.Y., 1953).

[2] H. Yamakawa, *Modern Theory of Polymer Solutions* (Harper, New York, 1971).

[3] C. Domb, Adv. Chem. Phys. 15, 229 (1969).

[4] P. G. de Gennes, Macromolecules 9, 587 (1976).

[5] P. H. Verdier and W. H. Stockmayer, J. Chem. Phys. 36, 227 (1962); F. Geny and L. Monnerie, Macromolecules 10, 1003 (1977).

[6] H. J. Hilhorst and J. M. Deutch, J. Chem. Phys. 63, 5153 (1975); H. Boots and J. M. Deutch, J. Chem. Phys. 67, 4608 (1977).

[7] J. G. Kirkwood, *Macromolecules* (Gordon and Breach, New York, 1976).

[8] D. E. Rouse, J. Chem. Phys. 21, 1272 (1953).

[9] D. E. Kranbuehl and P. H. Verdier, J. Chem. Phys. 67, 361 (1977).

[10] P. Debye, J. Phys. Colloid Chem. 51, 18 (1947).

[11] J. P. Cotton, D. Decker, B. Farnoux, G. Jannick, R. Ober, and C. Picot, Phys. Rev. Lett. 32, 1170 (1974).

[12] S. F. Edwards, Proc. Phys. Soc. 85, 613 (1965).

[13] D. E. Kranbuehl and P. H. Verdier, J. Chem. Phys. 56, 3145 (1972); P. H. Verdier, J. Chem. Phys. 59, 6119 (1973).

[14] D. Jasnow and M. A. Moore, J. Phys. (Paris) Lett. 38, L467 (1977).

Heat-Capacity Measurements of the Critical Coupling between Aluminum Grains

T. Worthington[a] and P. Lindenfeld

Serin Physics Laboratory, Rutgers University, New Brunswick, New Jersey 08903

and

G. Deutscher

Department of Physics, Tel-Aviv University, Ramat-Aviv, Israel

(Received 21 February 1978)

We have measured the heat capacity of granular aluminum specimens with normal-state resistivities ρ_N between 0.6×10^{-3} and 40×10^{-3} Ω cm. The specimens become superconducting with a heat-capacity transition which is BCS-like for the lowest ρ_N, and then diminishes until it is no longer observable for the highest ρ_N. We conclude that the grains become decoupled such that, because of their small size, they do not exhibit bulk superconductivity when they are isolated.

When aluminum is evaporated in the presence of oxygen it deposits in the form of metallic grains surrounded by insulating oxide. With increasing oxygen pressure the oxide barrier becomes thicker, the grains become increasingly decoupled, and the room-temperature normal-state resistivity ρ_N of the specimen increases. For ρ_N larger than 10^{-4} Ω cm the grain size remains constant at about 30 Å.[1,2]

We have made measurements on a series of granular aluminum films which show that the discontinuity in the heat capacity, which is characteristic of bulk superconductivity, is there to its full extent only in the specimen with the lowest

value of ρ_N (0.6×10^{-3} Ω cm). In the specimens with greater ρ_N the change in the heat capacity becomes smaller, and occurs at a lower temperature and over a wider temperature interval, until for the specimen with the highest value of ρ_N (40×10^{-3} Ω cm) it is no longer observable. We were thus able to show that when the grains are isolated they show no heat-capacity transition and that they are, therefore, smaller than the characteristic size below which bulk superconductivity cannot occur in isolated grains.[3-6] In addition, our results show that there is a rather narrow range of values of ρ_N, corresponding to a small change in composition,[7] such that on one side of